

COMBINED DELAMINATION AND MATRIX CRACKING IN ADAPTIVE COMPOSITE LAMINATES

Robert P. Thornburgh*

Vehicle Technology Directorate – Army Research Laboratory
NASA Langley Research Center
Hampton, VA 23681-2199

Aditi Chattopadhyay†

Department of Mechanical and Aerospace Engineering
Arizona State University
Tempe, AZ 85287-6106

ABSTRACT

An approach for modeling the response of laminated composite plates with piezoelectric patches, taking into account damage, is developed. An analytical model is presented that includes the effects of delamination and transverse matrix cracking. The equations of motion are formulated by using a coupled piezoelectric-mechanical theory that enables simultaneously solution for the mechanical strains and electric displacement. The finite element method is used with a refined, higher-order theory to model the composite plate response. Delamination is modeled by using a set of sublaminates, with continuity conditions that are enforced at the boundaries. Matrix cracking is incorporated as a reduction in ply stiffness that is a function of the crack density. Both matrix-crack closure and contact between the sublaminates are modeled, and a discrete time integration approach is used to compute the dynamic response. Results are shown for a simply-supported plate and illustrate the influence of composite damage on the electrical response of attached piezoelectric devices. The results demonstrate that this modeling technique approximates the influence of composite damage on the global response the damaged structure and predicts the transient electrical and mechanical response of piezoelectric smart composite structures.

INTRODUCTION

Composite laminates offer superior strength and stiffness over conventional materials for a given mass, but are also vulnerable to damage such as delamination and matrix cracking. This damage can occur during service life, as a result of low-velocity impact or

stresses created by excessive loading. The presence of delamination and matrix cracking is known to alter the dynamic characteristics and also reduce the strength of a structure, particularly under compressive loading. Thus, it would be beneficial to develop a means for detecting this type of damage in a composite structure.

The concept of using piezoelectric materials, in the form of thin actuators and sensors mounted to a structure, is being investigated by many researchers as a possible means for structural health monitoring and damage detection. The reduction in laminate stiffness caused by delamination and matrix cracking leads to changes in natural frequencies, mode shapes, damping and the strain field within a composite plate. Thus, the measurement of dynamic response using piezoelectric sensors appears to be a promising approach for detecting damage. Since experimental investigations can be expensive, damage detection research would benefit from an accurate and efficient computational model. To be of practical importance, the model must be capable of representing the effect of damage in composite structures with embedded or surface-bonded piezoelectric sensors, and must be capable of representing the impact of the damage on the dynamic structural and electrical response of the system. Because such matrix cracking is generally found with delamination resulting from fatigue or low-velocity impact, the combined modeling of delamination and matrix cracking is necessary for an accurate simulation of a damaged smart composite structure.

A large amount of literature has been published on modeling the effects of transverse matrix cracking on the stiffness degradation of composite laminates.¹⁻⁷ Matrix cracks open under load, thus creating an increase in the global strains of a laminate and a

* Aerospace Engineer, Mechanics and Durability Branch. Member AIAA.

† Professor. Associate Fellow, AIAA.

This material is a work of the U.S. Government and is not subject to copyright protection in the United States.

reduction in the effective stiffness. The cracked layer is still carrying some of the load, and thus the reduction in laminate stiffness is a function of crack density. Because damaged laminates usually contain hundreds of individual matrix cracks, most analytical models have represented the damage as an idealized arrangement of cracks spaced evenly apart, at an average distance. Solutions are then computed as functions of the average crack density. Some models are closed-form solutions,^{1,2} while others are parametric models based on matching experimental data. Early models were applicable to only pure extension, making them inappropriate for structures with complex loading. The behavior under shear loading was then addressed, and models that could be applied to angle-ply laminates were developed.^{1,2,4,6} Recently, models have been developed which combine simulation of the inplane stiffness degradation with the ability to estimate the changes in stiffness caused by bending loads.³⁻⁵ These models are capable of effectively simulating matrix cracking in a structure under dynamic loading, if the complications created by crack closure are addressed.

The majority of the work that has been conducted on delamination detection has concentrated on predicting delamination growth and the associated reduction in compressive strength of a structure subjected to quasi-static loading. Delamination also affects the dynamic response of a structure, yet there are fewer models for describing these effects.⁷⁻¹⁶ There have been very few efforts reported that attempt to accurately model the presence of both delamination and matrix cracking⁷ or address how these forms of damage influence the piezoelectric response of adaptive structural systems.^{14,15} The delamination also forms sublaminates that can come into contact with each other during plate vibration. This contact has been examined in only a few works,^{15,16} although the results from these works show that contact can sometimes have a significant influence on the dynamic response of a laminate. This lack of information is not surprising, because the contact between the sublaminates makes determining the response a nonlinear problem, which requires the use of special time-integration methods that treat the discontinuity in the plate stiffness.¹⁷

Review of the studies previously described indicates a need for an effective method for modeling the dynamic response of damaged composites with attached piezoelectric devices. Thus, the objective of this research is to develop a model that is capable of describing the effect of delamination and matrix cracking in a composite plate, of arbitrary laminate configuration, with consistent accuracy for a wide variety of laminate materials. The intention of this work is not to attempt to detect damage per se, but

rather, to illustrate a simulation technique that can be used to develop damage-detection methods and provide mechanics insight for future experimental efforts. While delamination, matrix cracking and piezoelectric structures have all been studied individually, in great detail, effort has not been made to combine them into a single model that is capable of capturing the effect of damage on the response of a smart structural system. This paper is an attempt to develop such a model by combining previous work on delamination,^{7,15} matrix cracking⁷ and piezoelectric modeling.^{15,18} Although, the assumptions made in modeling the damage yield approximate results, the model is very computationally efficient when compared to three-dimensional modeling of the damaged region, because exact characterization of each individual matrix crack is not required. This efficiency, combined with the versatility of the finite element method, results in a model that can potentially be used to study a vast number of structural configurations.

In the present paper, a coupled piezoelectric-mechanical model is combined with damage-modeling methods in order to predict the mechanical and electrical response of a damaged plate with piezoelectric actuators and sensors. First, the modeling of a plate with piezoelectric devices is described. The model uses a formulation based on simultaneous solution of the coupled piezoelectric-mechanical equations. Next, matrix cracking is incorporated into the structural model as a reduction in laminate stiffness, based on crack density. Delamination is then addressed by dividing the laminate into undelaminated regions and sublaminates, and modeling each as an individual plate joined together by continuity conditions. Included is a discussion on the influence of the delamination crack-tip singularity on the global response of the system and the appropriateness of neglecting it. A discontinuous time-integration technique is described, which can be used to investigate the effects of sublaminate contact on the dynamic response of the adaptive composite plate. Finally, results are presented to illustrate the models ability to simulate the effect of damage on the static and dynamic response of adaptive composite plates.

PIEZOELECTRIC MODELING

The model used in this paper is based on a recently developed, coupled piezoelectric-mechanical formulation, which allows accurate prediction of both the mechanical and the electrical response of a piezoelectric structural system.¹⁸ Traditionally, the constitutive relations used in structural analysis are expressed as a function of the components of the strain

(ϵ_{ij}) and electric (E_i) fields. Uncoupled models only solve one of the two constitutive equations depending on whether the piezoelectric device is being used as an actuator or a sensor. Use of the two-way coupled model allows both constitutive relations to be solved simultaneously, thus the transformation of energy within the piezoelectric material is more accurately represented. The model for smart composite laminates used in the present work is based on an alternate formulation of the constitutive relations given by

$$\sigma_{ij} = c^D_{ijkl}\epsilon_{kl} - h_{kij}D_k \quad (1)$$

$$E_i = -h_{ikl}\epsilon_{kl} + \beta^S_{ik}D_k \quad (2)$$

where the stress (σ_{ij}) and the electric field components (E_i) are related to the strains (ϵ_{kl}) and the components of the electric displacement (D_k) by the open-circuit elastic constants (c^D_{ijkl}), the zero-strain dielectric constants (β^S_{ij}) and the piezoelectric coefficients (h_{ijk}). Using this formulation, the electric displacement can be taken as constant through the thickness of the piezoelectric device, thus ensuring conservation of charge on each of the electrodes.

The equations of motion are formulated by using a variational approach based on Hamilton's Principle. The variational principle between times t_0 and t , for the piezoelectric body of volume V , are written in matrix form as

$$\delta\Pi = 0 = \int_{t_0}^t \int_V \left[\delta \left(\frac{1}{2} \rho \dot{\mathbf{u}}^T \mathbf{u} \right) - \delta \mathbf{H}(\boldsymbol{\epsilon}, \mathbf{D}) \right] dV dt + \int_{t_0}^t \delta \mathbf{W} dt \quad (3)$$

where the first term represents the kinetic energy, the second term is the electric enthalpy, and $\delta \mathbf{W}$ is the total virtual work done on the structure. The terms \mathbf{u} and ρ correspond to the mechanical-displacement vector and the density, respectively. The electric enthalpy, \mathbf{H} , is given in matrix-vector notation by

$$\mathbf{H}(\boldsymbol{\epsilon}, \mathbf{D}) = \frac{1}{2} \boldsymbol{\epsilon}^T \mathbf{C}^D \boldsymbol{\epsilon} - \boldsymbol{\epsilon}^T \mathbf{h} \mathbf{D} + \frac{1}{2} \mathbf{D}^T \boldsymbol{\beta}^S \mathbf{D} \quad (4)$$

Here, $\boldsymbol{\epsilon}$ and \mathbf{D} are used to represent the strains and the electric displacement vector, and \mathbf{C}^D , \mathbf{h} , and $\boldsymbol{\beta}^S$ are the matrices containing the elastic, dielectric and piezoelectric constants, respectively. The work done by body forces (\mathbf{f}_B), surface tractions (\mathbf{f}_S) and an electrical potential (ϕ) applied to the surface of the piezoelectric material is expressed as

$$\delta \mathbf{W} = \int_V \delta \mathbf{u}^T \mathbf{f}_B dV + \int_S \delta \mathbf{u}^T \mathbf{f}_S dS + \int_S \delta \mathbf{D}^T \phi dS \quad (5)$$

Equations (3-5) provide the basis for determining the equations of motion for a piezoelectric body.

A refined, higher-order laminate theory is used to model the mechanical-displacement field. This theory assumes a parabolic distribution of transverse-shear strain, thus providing accurate estimation of transverse-shear stresses for moderately thick laminates, with little increase in computational effort. Application of this theory to the equations of motion reduces the strains and displacements to five variables that are functions of the inplane coordinate only. The finite element method is then used to solve for these variables.

In the analysis presented herein, it is assumed that the piezoelectric material is oriented with its polarization axis normal to the mid-plane of the plate and that the piezoelectric device has electrodes covering its upper and lower surfaces. For this case, the electric displacement is zero along the two inplane coordinates. The out-of-plane electric displacement can then be discretized over the surface of the piezoelectric device by using finite elements.

By using these assumptions for the orientation of the piezoelectric device and the finite element method, the equations governing the response are used to solve for the nodal displacements and the nodal electric displacements. The equations only consider the mechanical aspects of the smart structure and neglect electrical inertia and damping. When considering an integrated, smart structural system, additional terms must be added to the system equations for electrical components in the system. For a simple LRC circuit, the variational energy, $\delta\Pi_q$, is given by

$$\delta\Pi_q = \delta \left(\frac{1}{2} L \dot{q}^2 \right) - \delta q R \dot{q} - \delta \left(\frac{1}{2C} q^2 \right) + V \delta q \quad (6)$$

where L , R and C are the inductance, resistance and capacitance, and V is the applied voltage. These equations can be combined with Eq. (3) to give the equations governing the response of both the piezoelectric body and the attached electrical system. The charge flow (q) in the electrical system equates to the integration of the electric displacement over the upper surface of the piezoelectric device. Since the finite element method has been used to discretize the electric displacement, the integration is transformed into matrix form using the matrix of interpolation functions (\mathbf{N}_q) and the nodal electric displacement (\mathbf{D}_e) as follows

$$q = \left(\int_S \mathbf{N}_q dS \right) \mathbf{D}_e = \mathbf{A}_q \mathbf{D}_e \quad (7)$$

Combining these equations, the resulting coupled electrical-mechanical system equations are obtained; that is,

$$\begin{bmatrix} \mathbf{M}_u & \mathbf{0} \\ \mathbf{0} & \mathbf{A}_q^T \mathbf{M}_q \mathbf{A}_q \end{bmatrix} \begin{Bmatrix} \ddot{\mathbf{u}}_e \\ \ddot{\mathbf{D}}_e \end{Bmatrix} + \begin{bmatrix} \mathbf{C}_u & \mathbf{0} \\ \mathbf{0} & \mathbf{A}_q^T \mathbf{C}_q \mathbf{A}_q \end{bmatrix} \begin{Bmatrix} \dot{\mathbf{u}}_e \\ \dot{\mathbf{D}}_e \end{Bmatrix} + \begin{bmatrix} \mathbf{K}_{uu} & \mathbf{K}_{ud} \\ \mathbf{K}_{du} & \mathbf{K}_{dd} + \mathbf{A}_q^T \mathbf{K}_q \mathbf{A}_q \end{bmatrix} \begin{Bmatrix} \mathbf{u}_e \\ \mathbf{D}_e \end{Bmatrix} = \begin{Bmatrix} \mathbf{F}_u \\ \mathbf{F}_D \end{Bmatrix} \quad (8)$$

where \mathbf{u}_e is the nodal displacements, \mathbf{D}_e is the vector containing the nodal electric displacements and any additional charge associated with the electrical system. The electric inductance, resistance and capacitance are contained in the \mathbf{M}_q , \mathbf{C}_q , and \mathbf{K}_q matrices, respectively. The matrix \mathbf{K}_{uu} is the mechanical-stiffness matrix, \mathbf{K}_{DD} is the electrical-stiffness matrix, and \mathbf{K}_{ud} and \mathbf{K}_{du} are the stiffness matrices due to piezoelectric-mechanical coupling. The vectors \mathbf{F}_u and \mathbf{F}_D are the force vectors due to mechanical and electrical loading. The matrix \mathbf{M}_u is the structural mass matrix, and to incorporate structural damping into the equations, a structural damping matrix \mathbf{C}_u is added to the system equations. The nature of the damping matrix can be chosen to meet the needs of the user, but in the present work classical damping is used.

MATRIX-CRACKING MODEL

The choice for the methodology used for modeling matrix cracking is dependent upon the overall purpose of the analysis and the structural model used. Unlike other studies that attempt to predict the amount of damage, based on loading history, it is assumed herein that the size and location of the damage is known. Thus, the micro-mechanics associated with crack growth are not included in the model used herein. The matrix cracking examined in this work consists of transverse matrix cracks that extend through the thickness of a ply and run parallel to the fibers. It is assumed that the cracking may be in any combination of layers, including the surface layers of the laminate. Matrix cracks cause a reduction in the structural stiffness by opening under load. If only the effects of Mode I and Mode III crack opening are included in the model, then the results would only be appropriate for classical-plate-theory models where transverse-shear deformation is not considered. For moderately thick plates modeled using a shear-deformation theory, the transverse shear contributes to the plate deflection, and therefore Mode II crack opening must be accounted for.

Some assumptions must be made to adequately model the effects of matrix cracking in a composite laminate. The first assumption is that the effects of the cracks on the global response can be modeled by a statistically

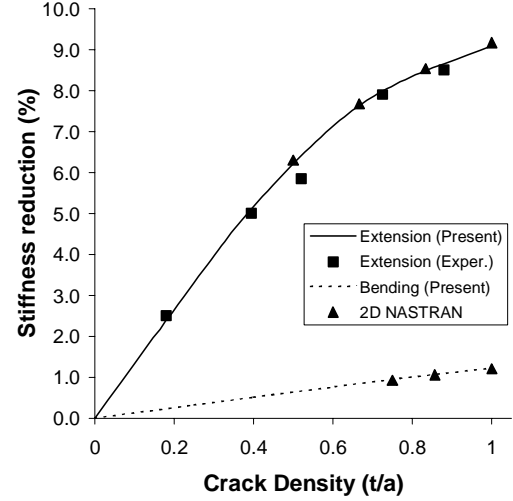


Fig. 1. Reduction in stiffness for graphite-epoxy $[0/90_2]_s$ laminate.

uniform array of cracks which are spaced at some average distance. It is also assumed that all cracks extend vertically through an entire layer and are aligned parallel to the fibers. The term “layer” is used with a special purpose in this section. Since consecutive plies oriented in the same direction have no means of arresting crack growth, which normally occurs when the crack tip intersects fibers running in a different direction, multiple plies with the same fiber orientation behave as a single, thick layer. As will be described later, it is also assumed that cracking in one layer is not influenced by the presence of cracking in other layers.

Since the equations of motion for the composite plate developed earlier in this work are based on the variation of the total energy, the effect of matrix cracking is incorporated as a reduced potential energy ($U_{cracked}$). This reduced potential energy is given by the difference between the strain energy in the uncracked laminate and the energy associated with the opening of a crack in the laminate (ΔU_{crack}) using

$$U_{cracked} = \int_A \left[\frac{1}{2} \boldsymbol{\varepsilon}^T \mathbf{C} \boldsymbol{\varepsilon} \right] dA - \Delta U_{crack} \quad (9)$$

The strain energy in the uncracked laminate is computed using the elastic stiffness matrix of the laminate, \mathbf{C} . Computing crack-opening energy at every stage of the finite element process would be a cumbersome and computationally expensive procedure. If a convenient method can be found for determining the crack-opening energy, then the effect of matrix cracking can be incorporated as an effective laminate stiffness ($\bar{\mathbf{C}}$) by using

$$U_{cracked} = \int_A \left[\frac{1}{2} \boldsymbol{\varepsilon}^T \overline{\mathbf{C}} \boldsymbol{\varepsilon} \right] dA \quad (10)$$

The energy associated with crack opening, assuming that the work done in one cracked layer is not affected by cracking in other layers, is defined as

$$\Delta U_{crack} = \sum_{k=1}^N \left\{ \int_A \left[\frac{1}{2} t^k \rho^k \boldsymbol{\tau}^k \mathbf{T} \boldsymbol{\beta}^{kk} \boldsymbol{\tau}^k \right] dA \right\} \quad (11)$$

The summation in this expression provides the total energy for all cracked layers. The energy is seen to be proportional to the thickness of the cracked layer, t^k , and the normalized crack-density parameter, ρ^k . The crack density is defined as the ratio of the thickness of the cracked layer to the average spacing between cracks, d^k ; that is,

$$\rho^k = \frac{t^k}{d^k} \quad (12)$$

The parameter, $\boldsymbol{\tau}^k$ represents the stresses that would be present in the uncracked laminate, which can in turn be related to the strain, $\boldsymbol{\varepsilon}$. The matrix, $\boldsymbol{\beta}^{kk}$, relates the stress to the crack opening energy and is dependent on the properties of both the cracked layer and the laminate as a whole. In the present work, finite element analysis of the representative crack is used to determine the $\boldsymbol{\beta}^{kk}$ matrix, as detailed in Ref. 7.

The method presented herein has been shown to accurately describe laminate stiffness degradation that is caused by matrix cracking.⁷ The reduction in extensional and bending stiffness for cracked $[0,90_2]_s$ laminates made of graphite-epoxy material is shown in Figure 1. In this figure, the results obtained using the model presented herein for both extension (solid line) and bending (dashed line) are compared with experimental data¹ and two-dimensional NASTRAN models,⁷ represented by the squares and triangles respectively. Unlike most closed-form solutions, this method gives excellent agreement for a variety of materials and ply layups, and also gives good results for inplane and transverse-shear stiffness. This versatility makes the model a valuable tool for estimating the stiffness degradation caused by matrix cracking when little experimental data is available.

DELAMINATION MODELING

To incorporate delamination into the structural model, the structure is divided into regions composed of individual sublaminates, and the variational equations, Eqs. (3-5), are applied to each region.¹⁵ Next,

continuity conditions are imposed at the interfaces between the undelaminated region and the sublaminates, based on the offset between the finite element nodes at the midplane of each sublaminate. The out-of-plane displacements, slopes and the inplane displacements are forced to be equal for the laminate and sublaminate on each side of the interface, resulting in a set of constraint equations. A transformation matrix is constructed in order to eliminate the degrees of freedom at the boundary of the sublaminates from the system matrices. This transformation condenses the system degrees of freedom along the boundary of the delamination to effectively remove the sublaminate nodes and reform the system equations in terms of the nodal degrees of freedom belonging to the undelaminated region. This approach is an effective and efficient method for modeling delamination, but two aspects of the delaminated plate that still need to be addressed are the crack-tip singularity and contact between the sublaminates.

Delamination Crack-Tip Singularity

By modeling the sublaminates as individual plates and directly connecting them, the singularity created by the delamination crack tip has been neglected. Likewise, most other models that have been used to describe the vibration of delaminated composite plates have also neglected this singularity. As a result, the localized strains and stresses in the vicinity of where the sublaminates join the undelaminated structure are not accurately modeled. Since the objective of this work is to capture the effect of delamination on the global response of the structure, this deficiency is not necessarily of concern, provided that this singularity does not create any large changes in the global deformation of the structure. The following discussion is presented to illustrate when this assumption applies.

To verify that the delamination crack-tip singularity has a minimal effect on the global structural deformation, an idealized two-dimensional delaminated beam was modeled. The beam, shown in Fig. 2, is cantilevered

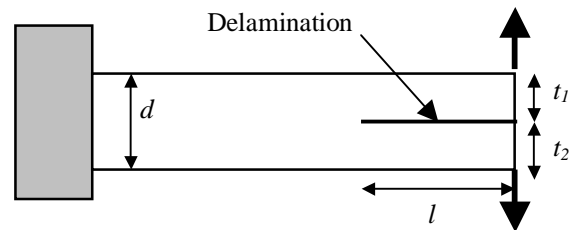


Fig. 2. Cantilevered beam for crack tip analysis.

and has a delamination starting at the free end. The beam was assumed to be made of an isotropic material to allow convenient finite element modeling. The beam was modeled by using a traditional mesh of two-dimensional plane-strain elements and, also, with a two-dimensional mesh that includes a finer mesh size and quarter-point crack-tip elements in the vicinity of the delamination tip. The sections on either side of the delamination are subjected to an opening force at the free end, and the resulting displacement (end opening) is computed for both finite element meshes. In the following results, the material was defined to have an elastic modulus of 91Gpa and a Poisson's ratio of 0.3. Figure 3 shows the two finite element meshes, in the deformed state.

An estimate of the effect of the singularity is calculated, based on the difference in end opening between the two finite element meshes ($\delta_1 - \delta_2$). These results are

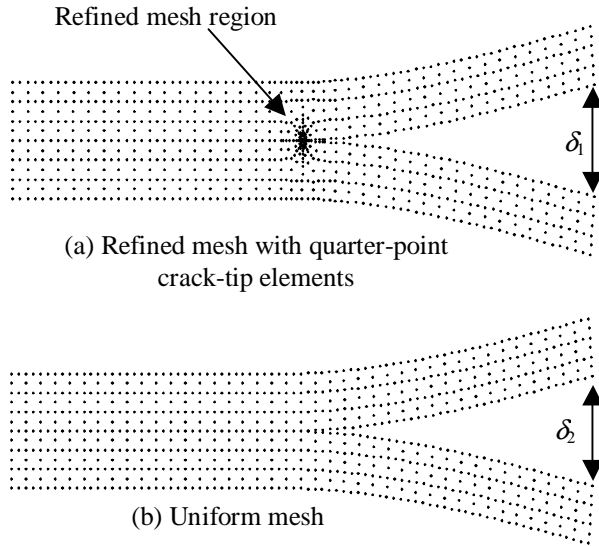


Fig. 3. Deformed shape of the finite element meshes

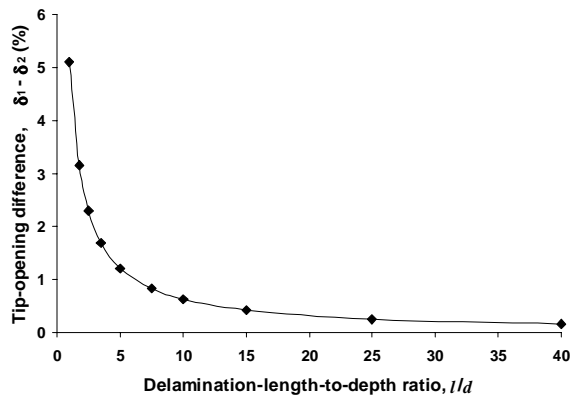


Fig. 4. Error from neglect of crack tip singularity.

presented in Fig. 4, for various delamination lengths, each denoted by the diamond symbols and connected by a solid line. For this case, the sublaminates are each 1mm thick, and the length of the undelaminated section is 1cm. In Fig. 4, the abscissa is the ratio of the length of the delamination, l , to the total beam depth, d . The results show that as the delamination becomes longer, the difference between the model with the singularity and the model without the singularity diminishes rapidly and that if the delamination is longer than about five times the thickness of the beam the difference is less than one percent. Thus, it is reasonable to neglect the crack-tip singularity provided the delamination length to laminate thickness is greater than five.

If the location of the delamination within the beam is changed to be closer to the top or bottom beam surface, similar results are obtained. The differences in delamination opening for three different delamination locations are shown in Figure 5. The diamonds, squares and triangles represent the results obtained for ratios of thickness of the upper sublaminate to the thickness of the lower sublaminate of 1, 0.5 and 0.25, respectively. These results show that the difference between the two models is the same, regardless of the location of the delamination within the thickness of the beam. Thus, the effect of the crack-tip singularity on the global deformation of the structure is governed more by its size relative to the thickness of the beam, as opposed to its depth from the surface. Because plate structures are generally thinner than beams, neglecting the crack-tip singularity in the plate model presented herein is not expected to create errors greater than approximately one percent, for all but the smallest of delaminations. Small delaminations would require a finer mesh of plate elements to model the small sublaminates, and a more accurate field description, through the thickness, may be necessary.

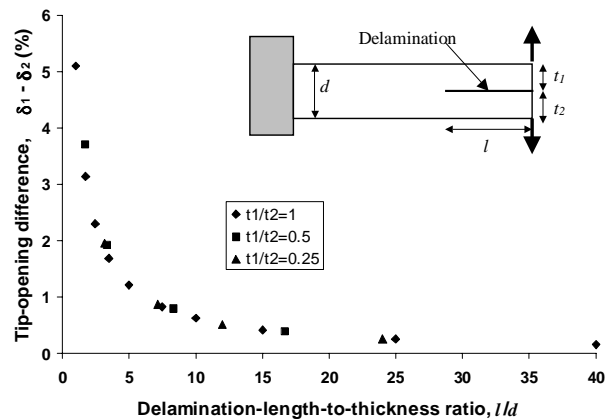


Fig. 5. Error from neglect of crack tip singularity for varying delamination locations.

Dynamic Contact

During vibration, contact occurs between the sublaminates in the delaminated region as the delamination opens and closes. The impact between the sublaminates affects the vibration response and should be incorporated into the developed plate model in order to accurately model the dynamic response of the plate. Mode shapes, obtained from a linear eigenvalue analysis, are not valid representations of the vibration of a delaminated plate due to the nonlinearity created by the contact between the sublaminates. For example, an eigenvector showing delamination opening during maximum deflection would also correspond to a condition where the sublaminates penetrate each other during the opposite deflection. As a result, the system cannot be represented by a linear combination of mode shapes, as in linear analysis, in order to allow computationally efficient determination of the transient response of the system.

Contact between sublaminates is modeled by using the procedure described in Ref. 15. That is, each node of the upper sublaminate is assumed to be connected to the corresponding node of the lower sublaminate by a fictitious spring. This spring is defined to have zero stiffness under tension and stiffness proportional to the transverse Young's modulus of the plate when subjected to compression. For analytical purposes, the stiffness matrix for the contact springs is formed as an independent matrix, and is based on the current nodal displacements. This stiffness matrix is then added to the linear stiffness matrix before solving for the nodal displacements. The use of fictitious springs is an easily implemented procedure that avoids recalculation of the positions and velocities of the sublaminates based on conservation of momentum each time contact or release occurs.¹⁶ The difficulty in using these springs during dynamic analysis is that the sudden change in stiffness of the springs acts like an impact, requiring careful modeling to correctly predict the response of the plate. Moreover, the bimodularity of the contact springs makes the transient problem nonlinear. In the present study, a time-integration technique was used to simulate the nonlinear response of the laminate when contact between the sublaminates is included.

The time-integration technique used in this paper is based on the discontinuous time-integration method of Cho and Kim.¹⁷ The reason for using this method, instead of a traditional Newmark method, is that the sudden change in stiffness that occurs during impact and release of the sublaminates creates jumps in the field variables that result in large numerical oscillations in the analytical solution. The discontinuous time-integration method uses a generalized derivative

concept to simulate the effect of sudden discontinuities that occur during contact and impact problems. The generalized derivative allows a discontinuity to be incorporated into a time-integration scheme without having any other constraints enforced on the nodes during contact and release. This time-integration method is an iterative solution algorithm, that uses a predictor-corrector approach for each time step. Further details about the discontinuous time-integration method are found in Ref. 17.

RESULTS FOR A DAMAGED PLATE

Much of the literature on the vibration of delaminated plates is primarily for cantilevered plates. Results are presented in this section that show the response of a carbon-epoxy composite plate, simply supported on all four sides and with damage in the form of both delamination and matrix cracking. The dimensions of the plate are 0.5m by 0.5m, the ply stacking sequence is $[0/90]_{2s}$, and the ply thickness is 0.127mm. The properties for the carbon-epoxy material are listed in Table 1. The plate was modeled by using a 20x20 finite element mesh. This mesh size was based on analysis that showed that this mesh size was able to accurately

Table 1. Properties of a carbon-epoxy lamina

E_{11}	134.4 GPa
E_{22}	10.34 GPa
G_{12}	5.00 GPa
ν	0.33
ρ	1.477 g/cm ³

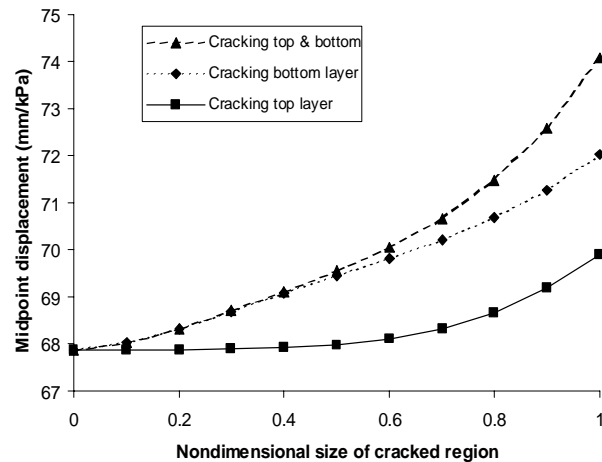


Fig. 6. Effect of matrix cracking on the static displacement of the square plate midpoint under uniform pressure.

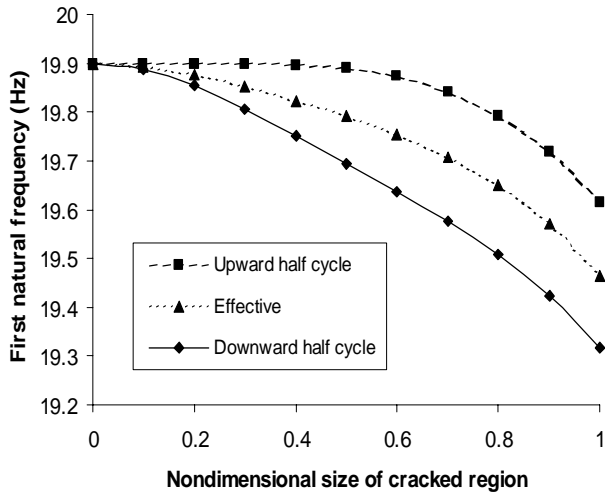


Fig. 7. Effect of matrix cracking on the square-plate fundamental frequency of vibration.

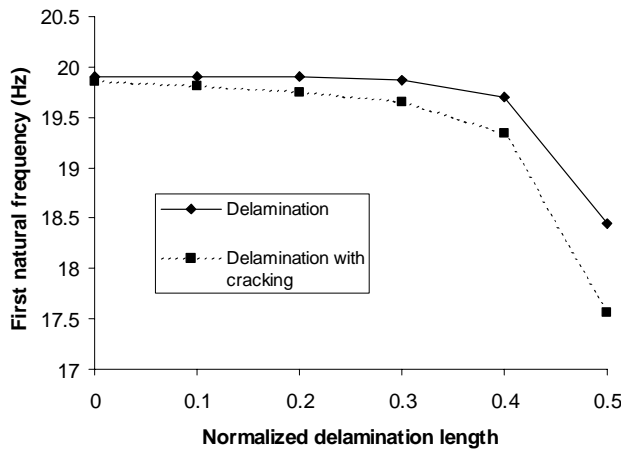


Fig. 8. Effect of delamination and matrix cracking on the natural frequency of the square plate.

predict the first twelve out-of-plane natural frequencies to within one-percent.

First, the effect of matrix cracking on the static response of the plate was examined for the case in which a uniform pressure was applied to the upper surface of the plate. The damage consisted of a square region of matrix cracking centered within the plane of the plate. The out-of-plane displacement at the center of the plate for a unit pressure is plotted in Fig. 6. These results are for the cases of cracking only in the bottom ply, cracking only in the topmost ply, and cracking in both the upper and lower plies. For all cases, a crack density of 1.0 was used.

The displacement per unit pressure is plotted in Fig. 6 against the non-dimensional size of the cracked region, which is defined as the ratio of the length of the cracked

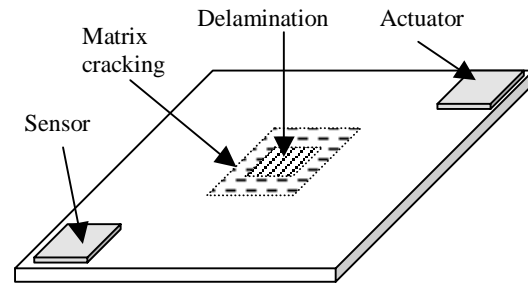


Fig. 9. Adaptive composite plate layout.

region to the length of the square-plate edge. The three cases presented are for cracking in the uppermost ply, denoted by the squares connected with a solid line, cracking in the lowermost ply, denoted by the diamonds connected with a finely dashed line, and cracking in both uppermost and lowermost plies, denoted by the triangles connected with a thick dashed line. The results show that cracking in the uppermost ply has less of an effect on the static deformation of the plate than cracking in the lowermost ply. This difference is because the pressure on the upper surface causes the cracks in the top ply to close, limiting their influence on the deformation. Although the cracks in the topmost ply are closed, some increase in the deflection is still induced since the cracking also reduces the shear stiffness of the ply. Since friction is neglected, the reduction in the shear stiffness is not affected by crack closure. The shear stresses are largest in the corners of the plate and as the cracked region grows larger and expands into the corners, the effect of the cracking on the plate deformation increases as expected.

Next, the linear eigenvalues for the plate with matrix cracking and delamination were studied to determine the effect of damage on the natural frequencies of the plate. The nonlinearity associated with crack closure and with contact between the sublaminates means that the system cannot be reduced by using modal analysis, but the eigenvalues still give a general indication about how much the damage is affecting the global response of the structure. The natural frequency for the first vibration mode is plotted against the size of the cracked region in Fig. 7. Cracking is in the bottom ply only, with a crack density of 1.0. The three curves represent the natural frequency for each half-cycle of the vibration and the effective frequency for the overall vibration of the plate. The downward half-cycle is represented by the diamonds connected with a solid line, the upward half-cycle is represented by the squares connected with a thick dashed line, and effective, or average, natural frequency is represented by the triangles connected with a finely dashed line. During the upper half-cycle, the cracks in the bottom ply are

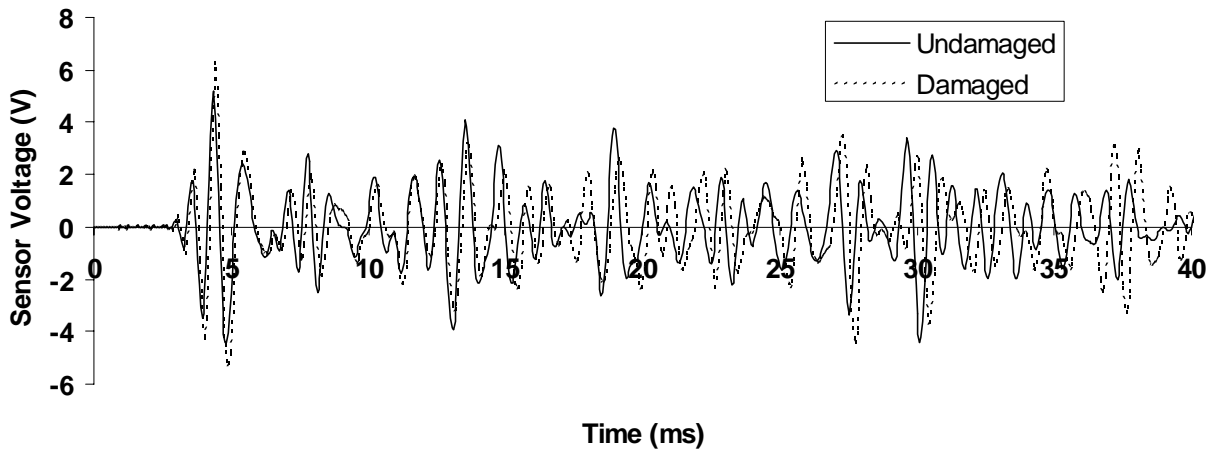


Fig. 10. Sensor voltage time history for a single cycle of 1000Hz actuator input.

closed and during the lower half-cycle they open, leading to different eigenvalues depending on the deformed shape at various times during the vibration. An effective vibration frequency is found by using the total period for one full cycle of the vibration to occur.

Figure 8 shows the natural frequency for a delaminated plate plotted against the ratio of delamination length to the edge length of the square plate. The two cases presented are for a plate with combined delamination and matrix cracking, represented by the squares connected with a finely dashed line, and for a plate with only delamination, represented by the diamonds connected with a solid line. The delamination is between the top two plies and forms a square region centered on the plate. For the case of combined delamination and matrix cracking, the cracking is in both the top and bottom plies, and extends 5cm beyond the delamination, as shown in Fig. 9. This damage pattern is approximately that which would result from a low-velocity impact on the back of the plate. For small delamination sizes, the fundamental natural frequency of the plate is reduced very little by the presence of the delamination, as has been shown by other research.⁸⁻¹⁰ Even for a delamination length of four-tenths of the length of the plate, the reduction in the natural frequency is only 1.0% for the delaminated plate and 2.7% for the plate with both delamination and matrix cracking. Higher frequency modes are not presented in this work, because they are greatly influenced by the local deformation associated with the delamination and the nonlinearity of sublaminar contact, making them less meaningful. These results indicate that except for extremely large delaminations, the effect of delamination and matrix cracking on the response of the plate is relatively small. The limited influence of the damage applies to both the static deformation and dynamic natural frequencies of the structure. This

limited influence can be viewed positively in that damage of the type considered herein will not result in drastic changes in the global response of system. In contrast, it also indicates that it is likely to be difficult to detect a small region of damage on a large structure using only the low frequency response.

Next, piezoelectric patches were used to study the response of the plate under dynamic loading conditions. The plate geometry shown in Fig. 9 was used as a representative adaptive structure. Piezoelectric patches of lead-zirconate titanate (PZT-5H) are located in opposite corners of the plate. The patches were 5cm by 5cm in area and 0.25mm thick. A 100V transient electrical voltage was applied to one patch and the opposite patch was used as a sensor to measure the global deformation response of the system. The sensor was assumed to be open circuited (zero net charge flow) and the voltage across the electrodes was used as the sensor output. The response of the system was simulated both with and without damage.

The first transient electrical signal simulated is a single cycle of a 1000Hz sine wave with 100V amplitude and numerical time integration was conducted using a 50 μ s time step. This signal generates an impulse type of response from the system. The time history of the sensor response is shown in Fig. 10 for both the undamaged plate (solid line) and the plate with a delamination and matrix cracking (dashed line). The damaged plate contains a 10cm by 10cm delamination between the top two plies, and the cracking is in both the top and bottom plies, extending 5cm beyond the delamination. The response of the two systems is quite similar when examined in the time domain and no apparent difference can be noted. The frequency-response curves for the systems are shown in Fig. 11. Here, small differences in the response of the system

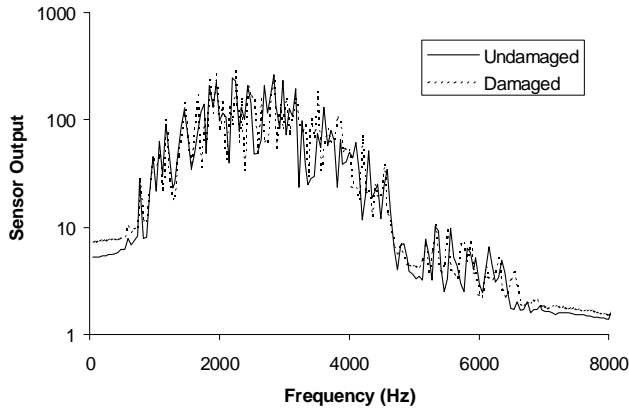


Fig. 11. Frequency response for a single cycle of 1000Hz actuator input.

are shown, due to the changes in the natural frequencies of the higher modes caused by the delamination and stiffness reduction associated with matrix cracking. The relative amplitude remains the same for both the damaged and undamaged cases and it would not be apparent which curve contained damage.

Next, an electrical signal with increasing frequency was applied to the system in which the input frequency increased linearly from 250Hz to 2000Hz, over the first 25ms of the simulation. Again, a $50\mu\text{s}$ time step was used for the numerical integration. The frequency response of the sensor voltage is plotted in Fig. 12 for the damaged (dashed line) and undamaged (solid line) laminates. As for the case of a single-cycle sine wave, only small differences in the response of the system are seen and the relative amplitude is similar for both the damaged and undamaged cases.

Finally, a continuous sine wave of 1000Hz was used as the electrical input. For this case, a $20\mu\text{s}$ time step was used. The resulting frequency-response curves are shown in Fig. 13. Again, the solid line represents the undamaged laminate and the dashed line represents the laminate with delamination and matrix cracking. These results suggest an increase in the damping of the structure due to the delamination and matrix cracking. This result is interesting, because only classical damping was included and friction between the sublaminates and matrix cracks was not modeled.

The present approach efficiently approximates the influence of delamination and matrix cracking on the response of composite laminates. Small changes were observed in displacement magnitudes and natural frequencies of the system at lower frequencies, while more noticeable changes occurred at higher frequencies, as seen by the shifting of the frequency-response peaks in Figs. 11 and 12. However, the cases

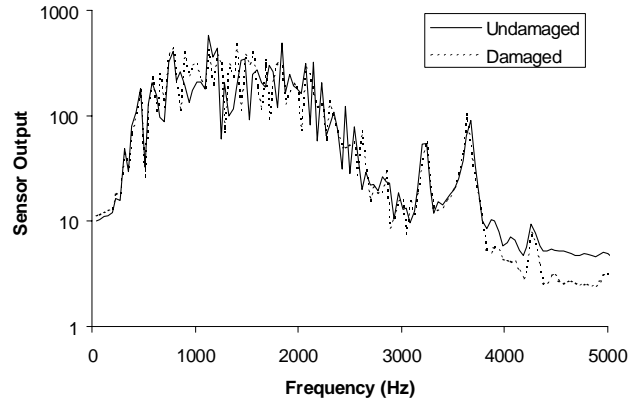


Fig. 12. Frequency response for a 250Hz to 2000Hz swept actuator input.

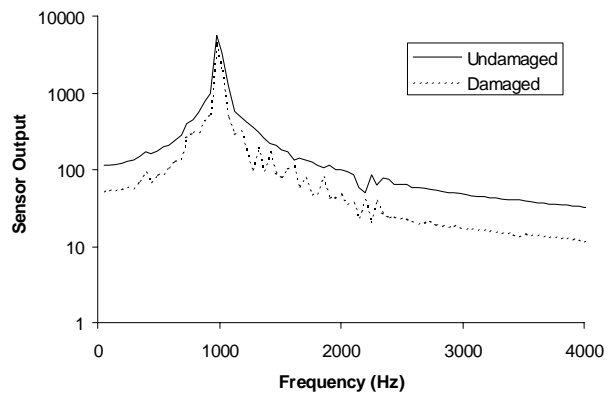


Fig. 13. Frequency response for a 1000Hz sinusoidal actuator input.

presented herein illustrate the difficulty of using low-frequency response to detect damage in composite laminates. Utilizing the higher frequencies for damage detection leads to other issues, due to the difficulty in accurately modeling the structural response for the higher modes. The present approach can be used with a more refined finite element mesh, but exact replication of the influence of the damaged region on the response at high frequencies is likely not possible as a result of the approximate nature of the model. However, damage is very probabilistic in nature and exact characterization of the damage would be of little avail since no two damaged regions would ever be identical. Thus, the model is still useful at higher frequencies, due to its ability to produce an effect that approximates that of an actual damaged region. This model will, therefore, be useful in simulating damage detection schemes utilizing piezoelectric sensors and actuators. However, an aspect that needs to be addressed in more detail is the attenuation of the vibrational response by the damaged region. The change in structural damping seems to be a major effect of delamination and matrix

cracking, and further investigation is needed to accurately model the damping in the damaged region.

CONCLUDING REMARKS

An approach has been developed to model the response of damaged composite plates with piezoelectric patches. Damage in the form of delamination and transverse matrix cracking has been included in the model. Delamination was incorporated by modeling the undamaged region and each sublaminates formed by the delamination as individual plates and then enforcing continuity conditions between them. Matrix cracking was included as a reduction in the laminate stiffness. The model utilizes a coupled piezoelectric-mechanical theory and finite elements to simultaneously solve for both the mechanical and electrical response of the system. Both matrix-crack closure and contact between the sublaminates are modeled, and a discrete time-integration approach was used to compute the dynamic response. The results demonstrate that this modeling technique does approximate the influence of composite damage on the global response the damaged structure and predicts the transient electrical and mechanical response of piezoelectric smart composite structures. Small changes in the displacement and global response at low frequencies were observed, along with moderate changes at higher frequencies. The change in the damping characteristics of damaged composite laminates appears to be a major effect of delamination and matrix cracking and requires further study and modeling.

REFERENCES

- 1) Allen, D. H. and Lee, J. -W., "Matrix Cracking in Laminated Composites Under Monotonic and Cyclic Loadings," *ASME, AMD*, Vol. 111, 1990, pp. 65-75.
- 2) Hashin, Z., "Analysis of Stiffness Reduction of Cracked Cross-Ply Laminates," *Eng. Fracture Mechanics*, Vol. 25, No. 5/6, 1986, pp. 771-8.
- 3) Makins, R. K. and Adali, S., "Bending of Cross-Ply Delaminated Plates With Matrix Cracks," *Journal of Strain Analysis for Engineering Design*, Vol. 26, No. 4, 1991, pp. 253-7.
- 4) Adolfsson, E. and Gudmundson, P., "Thermoplastic Properties in Combined Bending and Extension of Thin Composite Laminates With Transverse Matrix Cracks," *Int. J. of Solids & Structures*, Vol. 34, No.16, 1997, pp. 2035-60.
- 5) Smith, P. A. and Ogin, S. L., "On Transverse Matrix Cracking in Cross-Ply Laminates Loaded in Simple Bending," *Composites: Part A*, Vol. 30, No. 8, 1999, pp. 1003-8.
- 6) Tsai, C. -L. and Daniel, I. M., "The Behavior of Cracked Cross-Ply Composite Laminates Under Shear Loading," *Int. J. of Solids & Structures*, Vol. 29, No.24, 1992, pp. 3251-67.
- 7) Thornburgh, R.P. and Chattopadhyay, A., "Unified Approach to Modeling Matrix Cracking and Delamination in Laminated Composite Structures," *AIAA J.*, Vol. 39, No. 1, 2001, pp.153-60.
- 8) Tracy, J. J. and Pardoen, G. C., "Effect of Delamination on the Natural Frequencies of Composite Laminates," *J. of Composite Materials*, Vol. 23, 1989, pp. 1200-15.
- 9) Shen, M. -H. H. and Grady, J. E., "Free Vibration of Delaminated Beams," *AIAA J.*, Vol. 30, No. 5, 1992, pp. 1361-70.
- 10) Saravanos, D. A. and Hopkins, D. A., "The Effects of Delaminations on the Damped Dynamic Characteristics of Composite Laminates: Analysis and Experiments," *J. of Sound and Vibration*, Vol. 192, No. 5, 1996, pp. 977-93.
- 11) Williams, T. O. and Addressio, F. L., "A Dynamics Model For Laminated Plates With Delaminations," *Int. J. of Solids & Structures*, Vol. 35, Nos. 1-2, 1998, pp. 83-106.
- 12) Hou, J. P. and Jeronimidis, G., "Vibration of Delaminated Thin Composite Plates," *Composites: Part A*, Vol. 30, 1999, pp. 989-95.
- 13) Lu, X., Lestari, W. and Hanagud, S., "Nonlinear Vibrations of a Delaminated Beam," *J. of Vibration & Control*, Vol. 7, No. 6, 2001, pp.803-31.
- 14) Cao, A., Gabbert, U. and Poetzsch, R., "Delamination Modeling and Analysis of Adaptive Composites," *Proc. of AIAA/ASME/ASCE 39th Structures, Structural Dynamics, and Materials Conference*, 1998, Vol. 4, pp. 2911-6.
- 15) Thornburgh, R. P. and Chattopadhyay, A., "Modeling the Dynamic Effects of Delamination in Adaptive Composite Laminates," *Proceedings of AIAA/ASME/ASCE/AHS/ASC 43rd Structures, Structural Dynamics, and Materials Conference*, 2002, Vol. 3, pp.1944-54.
- 16) Kwon, Y. W. and Aygunes, H., "Dynamic Finite Element Analysis of Laminated Beams With Delamination Cracks Using Contact-Impact Conditions," *Computers & Structures*, Vol. 58, No. 6, 1996, pp. 1161-9.
- 17) Cho, J. Y. and Kim, S. J., "Discontinuous Time-Integration Method for Dynamic Contact/Impact Problems," *AIAA J.*, Vol. 37, No. 7, 1999, pp. 874-80.
- 18) Thornburgh, R. P. and Chattopadhyay, A., "Simultaneous Modeling of the Mechanical and Electrical Response of Smart Composite Structures," *AIAA J.*, Vol. 40, No. 8, 2002, pp. 1603-10.